10th World Congress on Structural and Multidisciplinary Optimization
May 19 - 24, 2013, Orlando, Florida, USA

Optimal design of the fiber-reinforcement to strengthen existing structures

Matteo Bruggi, Alberto Taliercio

Dept. of Civil and Environmental Engineering, Politecnico di Milano, Italy (matteo.bruggi@polimi.it, alberto.taliercio@polimi.it)

1. Abstract
An original approach is proposed to define the optimal design of any unidirectional fiber–reinforcement to improve the structural performance of existing structural elements. A problem of topology optimization is formulated, simultaneously searching for the regions to be strengthened and the optimal local fiber orientation. The maximum equivalent stress in the underlying material is minimized, for a given amount of reinforcement. The Tsai–Wu strength criterion is employed, to take into account the different strength properties of the material in tension and compression and the possible material anisotropy. Tensile stresses along the fiber direction are not allowed in the reinforcement. The resulting multi–constrained min–max problem is solved by mathematical programming. A numerical example is presented to discuss the features of the achieved optimal layouts, along with their possible application to the preliminary design of any fiber reinforcement.

2. Keywords: Topology optimization, Fiber-reinforcement, Orthotropic materials, Tsai-Wu failure criterion, Min-max problems.

3. Introduction
The use of Fiber Reinforced Composites (FRCs) for the strengthening of existing buildings has dramatically increased in the last decades. This technique has several advantages over standard retrofitting techniques such as flexibility, effectiveness, reversibility and reduced increase in structural weight [1]. Applications are equally found on historical masonry buildings and modern concrete or reinforced concrete members constructions. A suitable placement of unidirectional reinforcing strips provides structural elements with enhanced tensile strength, thus remarkably improving the load carrying capacity of the whole structure [2].

In this work a topology optimization problem is formulated to simultaneously search for the regions to be strengthened and for the optimal local inclination of the reinforcement. The fiber reinforcement modeled as an ad hoc orthotropic homogeneous medium, with mechanical properties depending both on the density and the orientation of the fibers [3, 4]. A min-max problem is formulated to minimize the local maximum equivalent stress in the underlying material, for a prescribed amount of fiber-reinforcement. With the aim of providing a quite general procedure for both isotropic (e.g. concrete) and orthotropic media (e.g. brickwork, reinforced concrete), the Tsai-Wu strength criterion is used to define an equivalent stress that efficiently detects highly tensile-stressed regions throughout the existing structural component. Since the compressive strength of the fibers is not relied on in practical retrofitting applications, a suitable set of relaxed stress constraints is introduced in the formulation. The resulting multi-constrained min-max problem takes full advantage of the implementation of an ad hoc selection strategy that allows the number of local stress evaluations to be significantly reduced, following the approach presented in [5].

A few numerical examples are presented to discuss the features of proposed procedure and the achieved optimal layouts, along with their possible application for the preliminary design of any structural retrofitting. Two-dimensional problems are analyzed, assuming the in-plane stiffness to be given by the sum of that of the fixed underlying layer and that of the overlying fiber-reinforcement. Extension to three-dimensional problems, where a two-dimensional overlapping layer has to be designed, are currently under investigations.

4. Governing equations
Consider a linear elastic material S occupying a two–dimensional domain Ω, either iso- or orthotropic; let C^{S0}_{ijhk} be the components of its 4th-order elasticity tensor. An orthotropic linear elastic layer F, representing any fiber-reinforcement, is superimposed on S; let C^{F}_{ijhk} be its elasticity constants. An orthogonal reference frame Ox_1x_2, hereafter referred to as 'global' reference frame, is adopted for both

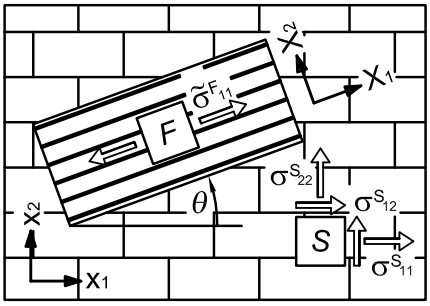

Figure 1: Portion of a structural element S retrofitted with a layer of fiber–reinforcement F.

layers, see Figure 1. As the optimal distribution and orientation of the reinforcing layer is sought, the dependence of C^F_{ijhk} on the fiber orientation $\theta(\chi)$ e.g. to axis x_1 ($0 \leq \theta < \pi$) and the density of the reinforcement material $\rho(\chi)$ ($0 \leq \rho \leq 1$) at any point $\chi \in \Omega$ are expressed as

$$C^F_{ijhk}(\rho(\chi), \theta(\chi)) = \rho(\chi)^p C^{F0}_{ijhk}(\theta(\chi)), \tag{1}$$

where the well–known SIMP model [6] has been adopted. $C^{F0}_{ijhk}(\theta(\chi))$ is the stiffness tensor for the 'virgin' medium; $p > 1$ is a penalization parameter (usually $p = 3$, see e.g. [7]).

Assuming perfect bonding, both layers share the same displacement field $\underline{u}$ in Ω. Over a part Γ_t of the boundary of Ω, tractions $\underline{t}_0$ are prescribed, whereas over the remaining part Γ_u displacements $\underline{u}^S_0$ are prescribed.

In matrix form, the relationship between the in-plane strain components ($\underline{\varepsilon} = [\varepsilon_{11}\, \varepsilon_{22}\, 2\varepsilon_{12}]$ and the in-plane stress components $\underline{\sigma}^S$ in the layer to be reinforced ($\underline{\sigma}^S = [\sigma^S_{11}\, \sigma^S_{22}\, \sigma^S_{12}]$) in the global reference frame can be expressed as $\underline{\sigma}^S = \mathbf{C}^{S0}\underline{\varepsilon}$, where

$$\mathbf{C}^{S0} = \frac{1}{1 - \nu^S_{12}\nu^S_{21}} \begin{bmatrix} E^S_{11} & \nu^S_{12}E^S_{11} & 0 \\ \nu^S_{21}E^S_{22} & E^S_{22} & 0 \\ 0 & 0 & G^S(1 - \nu^S_{12}\nu^S_{21}) \end{bmatrix}, \tag{2}$$

Here, E^S_{11}, E^S_{22} are the Young moduli, ν^S_{12}, ν^S_{21} are the Poisson's ratios and G^S is the in-plane shear modulus of the material to be reinforced (with $\nu^S_{12}E^S_{11} = \nu^S_{21}E^S_{22}$).

Similarly, let $\underline{\sigma}^F = [\sigma^F_{11}\, \sigma^F_{22}\, \sigma^F_{12}]$ be the array of the stress components in the reinforcing layer. Denote by X_1, X_2 the symmetry axes of the reinforcing material (see Fig. 1), hereafter referred to as 'local' reference frame. Assuming that the reinforcement exhibits prevailing stiffness along the fiber direction (X_1), the elastic matrix $\mathbf{C}^{F0}$ in the local reference frame reads

$$\mathbf{C}^{F0} = \begin{bmatrix} E^F & 0 & 0 \\ 0 & 0 & 0 \\ 0 & 0 & 0 \end{bmatrix} \tag{3}$$

where E^F is the Young modulus along the fiber direction. The array of the stress components in the local reference frame, $\widetilde{\underline{\sigma}}^F$, can be expressed as $\widetilde{\underline{\sigma}}^F = \mathbf{T}^{-1}\underline{\sigma}^F$, where $\mathbf{T}$ is the classical transformation matrix for the array of the stress components, depending on θ. In matrix form, the stress-strain law for the reinforcing layer in the global reference frame reads $\underline{\sigma}^F = \rho^p\, \mathbf{T}(\theta)\mathbf{C}^{F0}\mathbf{T}(\theta)^T\underline{\varepsilon}$. Note that, accordingly, the only non–vanishing stress component in the reinforcement is the normal stress along the fibers, $\widetilde{\sigma}^F_{11}$.

The weak formulation for the elastic equilibrium of the body can be stated as: find $\underline{u} \in H^1$ such that $\underline{u}\,|_{\Gamma_u} = \underline{u}^S_0$ and

$$\int_\Omega \underline{\varepsilon}(\underline{u})^T \left(\mathbf{C}^{S0} + \rho^p\, \mathbf{T}(\theta)\mathbf{C}^{F0}\mathbf{T}(\theta)^T\right) \underline{\varepsilon}(\underline{v})\, d\Omega \;=\; \int_{\Gamma_t} \underline{t}^S_0 \cdot \underline{v}\, d\Gamma, \tag{4}$$

$\forall \underline{v} \in H^1$. In the bilinear form on the l.h.s. in Eq. (4), the contribution of each material layer to the overall strain energy can be pinpointed.

To obtain a numerical approximated solution of the equilibrium problem, Ω is subdivided N quadrangular elements with bi–linear displacement shape functions. A piecewise constant discretization is adopted for the density field and the orientation field: from here onwards, x_e and t_e ($e = 1 \ldots N$) will

denote the values of ρ and θ in the $e-$th finite element, respectively. Eqn. (4) reduces to the following matrix form:

$$\sum_{e=1}^{N} \left[\mathbf{K}_e^{S0} + x_e^p \, \mathbf{K}_e^{F0}(t_e)\right] \; \mathbf{U} \; = \; \mathbf{F}, \tag{5}$$

where $\mathbf{K}_e^{S0}$ is the stiffness matrix of any element of the unreinforced structure, $\mathbf{K}_e^{F0}$ is the stiffness matrix of any element of the reinforcing layer, $\mathbf{U}$ is the array of the nodal degrees of freedom sand $\mathbf{F}$ is the array of the nodal equivalent loads.

In the formulation of the topology optimization problem for the reinforcing layer, the stress along the fiber direction, $\widetilde{\sigma}_{11}^F$, will be constrained to take only positive values all over Ω. Indeed, the poor performances of any thin FRC lamina in compression are well–known, as debonding and buckling phenomena can occur: the constraint ensures that the FRC strips act as distributed ties to strengthen any brittle structure against potential cracking and tensile failure. In a finite element formulation, this constraint will be expressed as

$$\widetilde{\sigma}_{e,11}^F = x_e^p \, \mathbf{L}_{F,e}(t_e) \, \mathbf{U}_e \geq 0, \quad e = 1 \dots N \tag{6}$$

where $\mathbf{L}_{F,e}$ is a 'failure stress matrix' depending on t_e, that recovers an equivalent stress for the fiber-reinforcing layer, in the e–th finite element, from the generalized displacement vector, $\mathbf{U}_e$.

Following [8], an appropriate failure criteria for the porous SIMP material should be defined on the so–called apparent 'local' stress $\langle \sigma_{e,11}^F \rangle = \widetilde{\sigma}_{e,11}^F / x_e^q$, with $q > 1$. In the numerical applications, the non-negativity constraint will be prescribed on $\langle \sigma_{e,11}^F \rangle$.

To take the different strength properties in tension and compression of the underlying layer S to be retrofitted, a Tsai-Wu strength criterion will be employed [9], which, in the 2D-case, reads:

$$\sigma_{eq}^S = F_1 \, \sigma_1 + F_2 \, \sigma_2 + F_{11} \, \sigma_1^2 + F_{22} \, \sigma_2^2 + 2F_{12} \, \sigma_1 \sigma_2 + F_{66} \, \sigma_{12}^2 \leq 1. \tag{7}$$

The Voigt notation has been used to denote the stress components ($\sigma_1 = \sigma_{11}$, $\sigma_2 = \sigma_{22}$, $\sigma_6 = \sigma_{12}$) referred to the local axes. F_i and F_{ij} $(i, j = 1, 2, 6)$ are material constants that may be expressed in terms of compressive strength values (σ_{L1c}, σ_{L2c}), of the tensile strength values (σ_{L1t}, σ_{L2t}), and of the in-plane shear strength σ_{Ls} along the local axes as follows:

$$\begin{aligned} &F_{11} = -\frac{1}{\sigma_{L1t} \cdot \sigma_{L1c}}, \quad F_{22} = -\frac{1}{\sigma_{L2t} \cdot \sigma_{L2c}}, \quad F_1 = \frac{\sigma_{L1t} + \sigma_{L1c}}{\sigma_{L1t} \cdot \sigma_{L1c}}, \\ &F_2 = \frac{\sigma_{L2t} + \sigma_{L2c}}{\sigma_{L2t} \cdot \sigma_{L2c}}, \qquad 2F_{12} = -\sqrt{F_{11} F_{22}}, \qquad F_{66} = \frac{1}{\sigma_{Ls}^2}. \end{aligned} \tag{8}$$

In particular, if the layer to be reinforced is isotropic, setting $\sigma_{Lc} = \sigma_{L1c} = \sigma_{L2c}$, $\sigma_{Lt} = \sigma_{L1t} = \sigma_{L2t}$ and $F_{66} = 3/(\sigma_{L1t} \cdot \sigma_{L1c})$, the Tsai–Wu criterion can be reduced to a parabolic strength criterion of the form:

$$\sigma_{eq}^S = \frac{3J_2'}{\sigma_{Lc} \cdot \sigma_{Lt}} + \frac{\sigma_{Lc} - \sigma_{Lt}}{\sigma_{Lc} \cdot \sigma_{Lt}} J_1 \leq 1, \tag{9}$$

where J_1 is the first stress invariant and J_2' is the second invariant of the deviatoric stress (see e.g. [10]).

In a finite element formulation, Eq. (7) (or (9)) can be rewritten as:

$$\sigma_{e,eq}^S = \mathbf{U}_e^t \, \mathbf{Q}_{S,e} \, \mathbf{U}_e + \mathbf{L}_{S,e} \, \mathbf{U}_e \leq 1, \quad e = 1 \dots N, \tag{10}$$

where $\mathbf{Q}_{S,e}$ and $\mathbf{L}_{S,e}$ are 'failure stress matrices' that recover the quadratic and the linear part of the Tsai–Wu equivalent stress for the existing structure, in the e–th finite element, from the generalized displacement vector of the element.

5. The topology optimization problem

Aim of the proposed approach is distributing a limited amount of fiber–reinforcement, that has to be properly oriented to minimize the maximum value of the equivalent Tsai–Wu stress measure σ_{eq}^S over the existing structure. Taking Eqs. (5), (6) and (10) into account, the discrete stress–constrained formulation

can be cast in the following form:

$$\begin{cases} \min\limits_{x_e,t_e} & \max\limits_{e=1,N} \left\{\sigma^S_{e,eq}\right\} \\ \text{s.t.} & \sum_{e=1}^{N} \left[\mathbf{K}_e^{S0} + x_e^p\, \mathbf{K}_e^{F0}(t_e)\right]\ \mathbf{U} \ = \ \mathbf{F}, \\ & \sum_N x_e V_e \ / \ \sum_N V_e \ \leq \ V_f, \\ & x_e^{(p-q)}\ \overline{\sigma}^F_{e,eq}(t_e) \geq 0, \qquad \text{for} \quad e = 1, ..., N \\ & 0 \leq x_e \leq \ 1, \\ & 0 \leq t_e < \ \pi. \end{cases} \tag{11}$$

The first inequality constraint in Eq. (11) defines the available amount of reinforcement, V_f; the weight of the FRC layer is given by sum of the products of the element density x_e by the relevant volume V_e over the N finite elements.

The problem in Eq. (11) is handled via mathematical programming, resorting to the Method of Moving Asymptotes (MMA) [11] as minimizer. The min–max problem is solved writing a minimization problem where the constraints in Eqn. (11.2–4) are preserved along with the optimization unknowns and their range of variations, while a new scalar objective function is considered, see in particular [12].

To improve the computational performance of the proposed approach, a very limited set of $\sigma^S_{e,eq}$-values is passed to the minimizer rather than the N entries, meaning that a check of the highly–stressed regions is performed in the underlying layer, see also [13]. In the retrofitting problems that are commonly dealt with, the elements that are responsible for the tensile failure of the underlying structure are located in limited regions of the domain and their set remains more or less unchanged during the optimization.

Referring to the constraints on $\sigma^F_{e,11}$, an alternative strategy has been implemented. Only the N^F_a constraints in Eqns. (11.3) whose l.h.s. is larger then 0.65 are considered to be active during the first iteration. The threshold is linearly increased until the tenth step and is constantly set to 0.85 thereafter, see also [5]. A very limited set of active constraints is able to steer the minimizer towards optimal solutions that are free from the arising of undesired compressive–stressed regions of reinforcement.

6. Numerical application

To illustrate the potentialities of the proposed approach, the optimal reinforcement of an architrave connecting two vertical elements and subjected to horizontal actions is sought, see Figure 2. A distributed shear load f =50 kN/m acts upon the structure.

The adopted discretization consists of regular meshes of square elements. The FRC layer to be optimized has a thickness $th^F = 0.15$ mm and an elastic modulus $E^F = 230$ GPa. The admissible volume fraction of reinforcing material $V_f = 0.15$. The optimization procedure is performed starting from an initial guess, where reinforcement is supposed to be evenly distributed over the structure, i.e. $\tilde{x}_e = V_f$ everywhere. Fibers are initially oriented according to the local direction of the largest principal stress in the unreinforced existing material.

A first investigation is performed assuming the architrave to be made of (isotropic) plain concrete with the following properties: $E^S_{11} = 21000$ MPa, $\nu^S_{12} = 0.21$, $\sigma_{L1t} = 1.5$ MPa, $\sigma_{L1c} = 20 \cdot \sigma_{L1t}$.

The optimal layout of the reinforcement is shown in Figure 3(a). The optimal fiber direction is approximately parallel to the FRP strips that can be identified by Figure 4. Inclined strips strengthen the critical corners of the architrave and span over the vertical elements up to the outer edges. There, the orientation of the reinforcement is mainly vertical and extended up to the ground constraints, thus

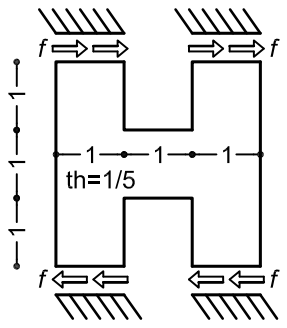

Figure 2: Architrave subjected to horizontal loads: geometry and boundary conditions.

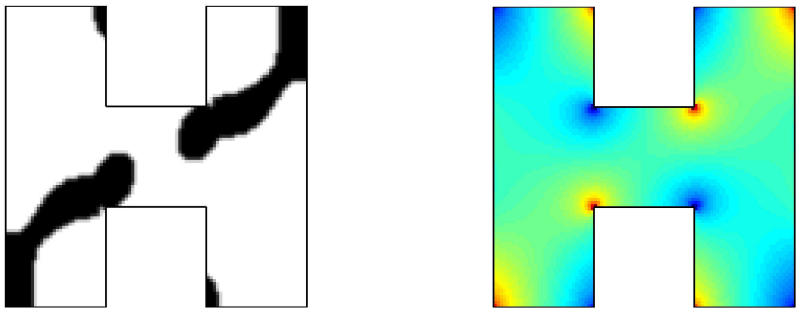

(a) (b)

Figure 3: Architrave made of plain concrete: optimal fiber–reinforcement for $V_f = 0.15$ (a) and contour plots of the equivalent stress $\sigma^S_{e,eq}$ over the element to be reinforced (b).

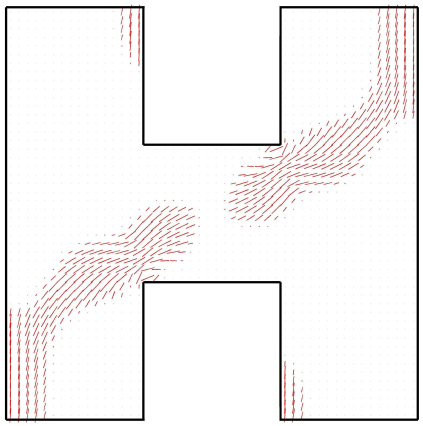

Figure 4: Architrave made of plain concrete: fiber orientation of the optimal reinforcement.

resisting the normal bending stresses. Minor regions of reinforcement are found along the inner edges of the vertical elements subjected to tensile stresses. A map of the equivalent stress measure σ^S_{eq} is plotted in Figure 3(b), where red spots stand for dangerous stress peaks.

A second investigation is performed assuming the architrave to be made of reinforced concrete. The material is isotropic as far as its elastic properties are concerned, which are given the values employed in the previous case. The strength anisotropy of the material is taken into account assuming $\sigma_{L2t} = 20 \cdot \sigma_{L1t}$; the remaining strength properties are the same of the plain concrete model.

The optimal reinforcing layout is shown in Figure 5(a), and suggests the adoption of an inclined reinforcement strip running through the architrave and connecting the critical corners shared with the vertical elements, see also Figure 6. The regions to be strengthened are not limited to highly stressed zones, but extend into the bulk of the coupled elements to provide an effective path for the tensile stresses arising from the applied shear loads. This is in agreement with results of the theoretical and experimental literature of aseismic design, see e.g. [14]. According to the contours of the equivalent stress measure σ^S_{eq} plotted in Figure 5(b), unlike the previous case the normal bending stresses arising in the vertical elements are not critical, because of the strength anisotropy of the underlying structure. This explains the difference between the optimal layouts obtained in the two cases (compare Figs. 3a and 5a).

The convergence plots for the two cases are shown in Fig. 7. In both cases the optimizer solves the multi–constrained min–max problem achieving optimal results through a smooth convergence. Apparently, the anisotropic Tsai–Wu model implies an increased computational cost respect to the isotropic parabolic strength criterion.

7. Concluding remarks

An original formulation based on topology optimization was proposed, to spot out the regions of any structural element which have to be strengthened by a given quantity of FRC to keep the stress below a

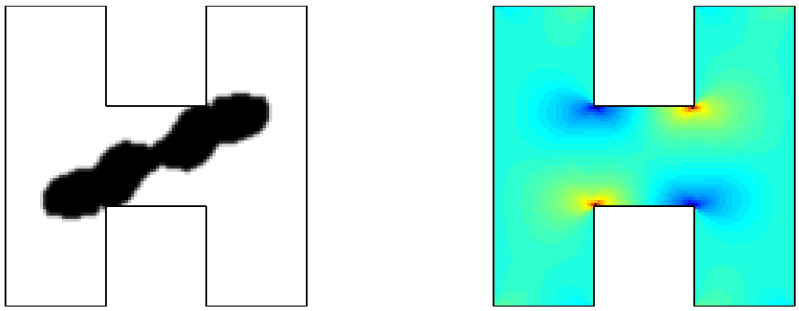

(a) (b)

Figure 5: Architrave made of reinforced concrete: optimal fiber–reinforcement for $V_f = 0.15$ (a) and contour plots of the equivalent stress $\sigma^S_{e,eq}$ over the element to be reinforced (b).

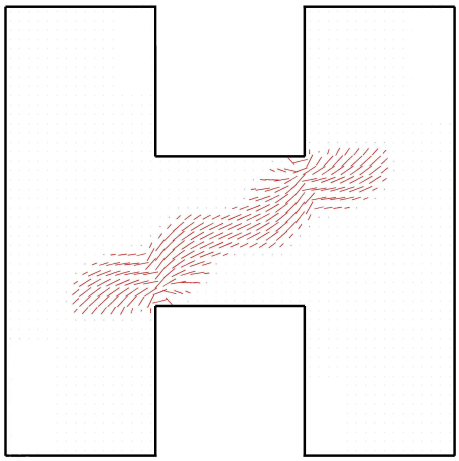

Figure 6: Architrave made of reinforced concrete: fiber orientation of the optimal reinforcement.

given threshold, while simultaneously defining the optimal inclination of the unidirectional reinforcement pointwise. The anisotropy of the reinforcing layer was taken into account, along with the different properties in tension and compression of the unreinforced material. A set of relaxed stress constraints was incorporated in the formulation to avoid compressive stresses in the reinforcement.

Numerical simulations have been presented to assess the capabilities of the proposed approach. The obtained solutions can inspire enhanced arrangements of the reinforcing strips. It was found that the optimal orientation of the reinforcing fibers can differ from that of the maximum principal stress in the underlying structure. The possible anisotropy of the underlying material also affects the layout of the optimal reinforcement.

In the current version, perfect bonding was assumed at the interface between FRC and underlying structure. Indeed, in practical applications an anchorage length must be provided, according to the prescriptions given by the technical codes, to allows tensile stresses to be gradually transferred from the ends of the reinforcing strips to the underlying structural layer. Also, the possibility of debonding should be considered. According to international standards, this can be managed by additional constraints on the stress in the FRC layer. This point will be addressed in the continuation of the research, where the extension of the proposed approach to the retrofitting of 3D structural elements will also be dealt with.

References

[1] C.E. Bakis, L.C. Bank, V.L. Brown, E. Cosenza, J.F. Davalos, J.J. Lesko, A. Machida, S.H. Rizkalla, T.C. Triantafillou, Fiber-reinforced polymer composites for construction - state-of-the-art review. *J. Compos. Constr.* 6, 73-87, 2002.

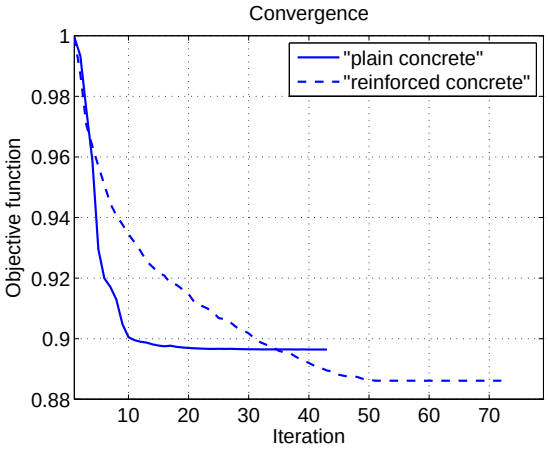

Figure 7: Optimal fiber–reinforcement for $V_f = 0.15$: convergence plots for plain concrete and reinforced concrete elements.

[2] J. Kato, E. Ramm, Optimization of fiber geometry for fiber reinforced composites considering damage. *Finite Elem Anal Des* 46,401-415, 2010.

[3] N. Pedersen, On optimal orientation of orthotropic materials. *Struct. Optim.* 1, 101-106, 1989.

[4] H.C. Cheng, N. Kikuchi, An improved approach for determining the optimal orientation of orthotropic material. *Struct. Optim.* 8, 101-112, 1994.

[5] M. Bruggi, P. Duysinx, Topology optimization for minimum weight with compliance and stress constraints. *Struct. Multi. Optim.* 46, 369-384, 2012.

[6] M.P. Bendsøe, N. Kikuchi, Generating optimal topologies in structural design using a homogeneization method. *Comp Meth Appl Mech Eng* 71, 197-224, 1988.

[7] M. Bendsøe, O. Sigmund, Material interpolation schemes in topology optimization. *Arch Appl Mech* 69, 635-654, 1999.

[8] P. Duysinx, M.P. Bendsøe, Topology optimization of continuum structures with local stress constraints. *Int J Numer Methods Eng* 43, 1453-1478, 1998.

[9] S.W. Tsai, E.M. Wu, A general theory of strength for anisotropic materials. *J Compos Mater* 5, 58-80, 1971.

[10] A. Taliercio, P. Sagramoso, Uniaxial strength of polymeric-matrix fibrous composites predicted through a homogenization approach. *Int Journ Solids Structures* 32, 2095-2123, 1995.

[11] K. Svanberg, Method of moving asymptotes - A new method for structural optimization. *Int J Numer Methods Eng* 24, 359-373, 1987.

[12] K. Brittain, M. Silva, D.A. Tortorelli, Minmax topology optimization. *Struct Mult Optim* 45, 657–668, 2012.

[13] R.T. Haftka, Z. Gürdal, Elements of structural optimization, third revised and expanded edition, Dordrecht, Kluwer Academic publishers, 1992.

[14] R. Park, T. Paulay, Reinforced Concrete Structures. Wiley, New York, 1975.